# Evaluation of New Actuators in a Buffet Loads Environment

Robert W. Moses*[a], Carol D. Wieseman[a], Aaron A. Bent[b], and Alessandro E. Pizzochero[b]
[a]NASA Langley Research Center, [b]Continuum Control Corporation

## ABSTRACT

Ongoing research in buffet loads alleviation has provided an application for recently developed piezoelectric actuators capable of higher force output than previously existing actuators could provide and that can be embedded within the vehicle's structure. These new actuators, having interdigitated electrodes, promise increased performance over previous piezoelectric actuators that were tested on the fin of an F/A-18 aircraft. Two new actuators being considered by the United States Air Force to reduce buffet loads on high performance aircraft were embedded into the fins of an F/A-18 wind-tunnel model and tested in the Transonic Dynamics Tunnel at the NASA Langley Research Center. The purpose of this test program, called ENABLE (Evaluation of New Actuators in a Buffet Loads Environment), was to examine the performance of the new actuators in alleviating fin buffeting, leading to a systems-level study of a fin buffet loads alleviation system architecture being considered by the USAF, Boeing, and NASA for implementation on high performance aircraft. During this wind-tunnel test, the two actuators performed superbly in alleviating fin buffeting. Peak values of the power spectral density functions for tip acceleration were reduced by as much as 85%. RMS values of tip acceleration were reduced by as much as 40% while using less than 50% of the actuators' capacity. Details of the wind-tunnel model and results of the wind-tunnel test are provided herein.

Keywords: Buffet Loads Alleviation, Smart Structures

## 1. INTRODUCTION

For high performance aircraft, such as the F/A-18, at high angles of attack, vortices emanating from wing leading edge extensions (LEX) on both sides of the aircraft often burst, immersing the vertical tails in their wake (Figure 1a). Although these vortices create lift, the resulting buffet loads on the vertical tails are a concern from airframe fatigue and maintenance points of view. Wind-tunnel and flight tests[1-11] have been conducted to quantify the buffet loads on the vertical tails of the F-15, F/A-18, and F-22. These tests were designed to characterize the flow mechanism and to quantify the buffet (unsteady differential pressures) acting on the vertical tails during high-angle-of-attack conditions.


(a) (b)

Figure 1. Flow Visualizations of Vortex from the LEX Bursting ahead of the Vertical Tail on an F/A-18 (Photographs Courtesy of the NASA Dryden Flight Research Center)

As shown in Figure 1b for the F/A-18, the source of the buffet stems solely from one dominant LEX vortex that bursts ahead of the vertical tails. In comparison, for the F-15 and F-22 configurations, the buffet is created by the combination of several vortices originating from the engine inlet and the wing leading edge as indicated by the trajectories shown in Figures 2a and

*r.w.moses@larc.nasa.gov; phone 1 757 864-7033; fax 1 757 864-8678; http://sonicboom.larc.nasa.gov; NASA Langley Research Center, Mail Stop 340, Hampton, VA 23681-2199

2b, respectively. Because the configurations of these vehicles differ, the corresponding vortices and their frequency contents also differ. As a result, worst-case fin buffeting (the responses of the fin to the unsteady differential pressures) occurs in different structural modes. Thus, geometric configuration of the aircraft plays a vital role in both the buffet (unsteady aerodynamics) and buffeting (structural response) of the fins.

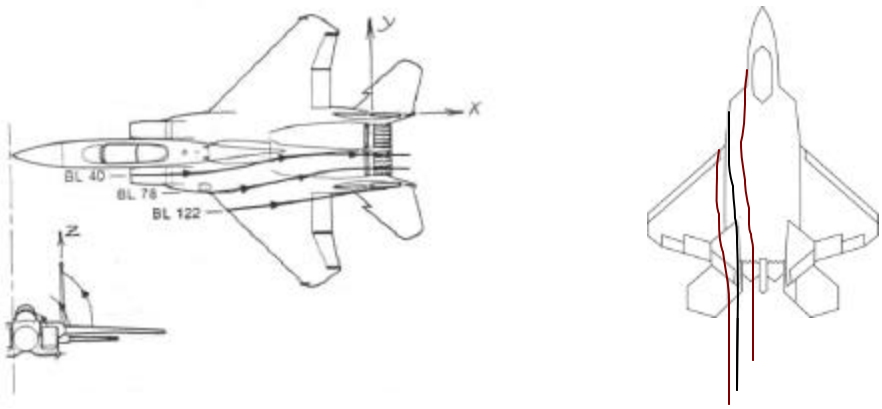


(a) F-15 Eagle (from Triplet et. al.) (b) F-22

Figure 2. Typical Trajectories of the Flow Affecting the Vertical Stabilizers

With the intent of lowering fin buffet loads, and thereby increasing fatigue life, a limited amount of research[5] has been aimed at modifying the vortices. However, because the vortices are needed to provide lift at high angles of attack, modifying them may solve one problem but may create another. Instead, efforts have been focused on controlling the structural response[11-16]. Three wind-tunnel tests[11, 13, 14] have implemented a variety of rudder and piezoelectric actuator concepts for buffet loads alleviation (BLA). Results of these tests illustrated the capabilities of the rudder to alleviate buffeting in the fin first bending mode and the piezoelectric actuators to alleviate buffeting in both the fin first bending and fin first torsion modes.


Figure 3. Full-scale Retired F/A-18 Ground Test Article
(Photo Courtesy of the Australian Aeronautical and Maritime Research Laboratory)

A full-scale ground test[15, 16] was conducted to assess the capabilities of piezoelectric actuators bonded to the outer surfaces of the fin (Figure 3) to alleviate "buffeting" due to simulated unsteady differential pressures. The results of the full-scale ground test indicated the need to develop a more efficient piezoelectric actuator. The piezoelectric actuators available at the time and implemented in these investigations[11, 13-16] consisted of piezoelectric plates with electrodes of opposite polarity placed on opposite faces of the plates. The plates were poled electrically through the thickness. When voltage was applied through the thickness of the plate, the plate would strain in its plane (i.e., $d_{31}$). This mechanism for strain is not as efficient as poling the plates in the plane of the actuator where the strain is desired (i.e., $d_{33}$). A follow-on full-scale ground test program, led by the USAF with participation of researchers from Boeing, NASA, Australia, and Canada, is underway to examine these more efficient actuators using the same test aircraft shown in Figure 3.

The purpose of the research program, called ENABLE (Evaluation of New Actuators in a Buffet Loads Environment), presented herein, is to examine qualitatively the performance of two new actuators that operate in the more efficient manner (i.e., $d_{33}$), leading to a systems-level study of a fin BLA system architecture being designed by Boeing for the follow-on full-scale ground test mentioned above. Based on published free-strain performance capabilities, the actuators chosen for this investigation are the Macro-Fiber Composite actuator[17] developed at the NASA Langley Research Center (LaRC-MFC™) and the Active Fiber Composite actuator[18, 19] developed at the Continuum Control Corporation (C3 AFC). Shown in Figure 4, representative performance capabilities of the LaRC-MFC™ and C3 AFC actuators ("Current Generation") were compared with those of several commercial actuator products ("Previous Generation")[17]. Defined by the strain and stress actuation capabilities of the device, the triangular region below each line approximately indicates the performance capability of each actuator. The data for the LaRC-MFC™ actuators were obtained from experimental free-strain measurements, with stresses extrapolated from the stiffness properties of the devices. The performance envelopes of the other devices were estimated from company promotional product literature. As seen in Figure 4, the strain and stress actuation capabilities of the "Current Generation" actuators compare very favorably with the "Previous Generation" actuators that were used in the previous BLA (wind-tunnel and ground) tests described above. The main objectives of this investigation are 1) to obtain data for verifying mathematical models and analyses of these actuators when embedded in the fin model, and 2) to study these actuators as components of a BLA system for providing guidance during the design phase of the systems-level study mentioned above.

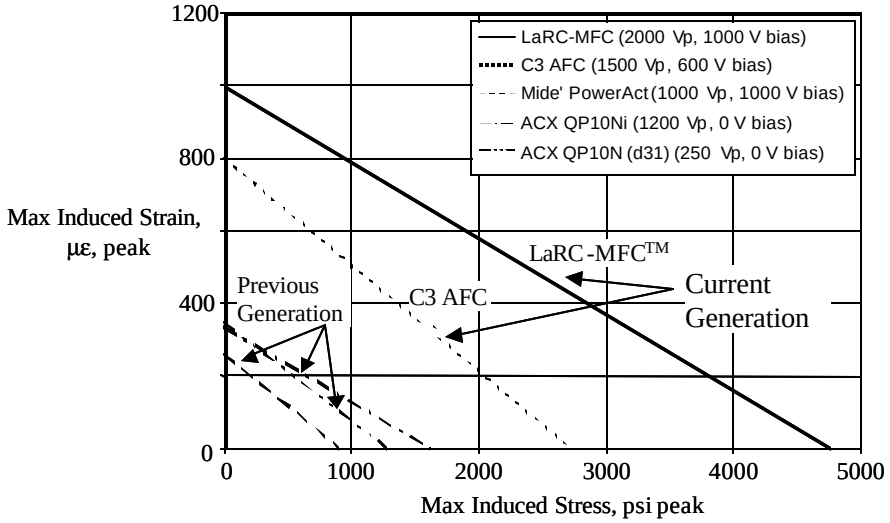


Figure 4. Relative Performance Envelope Comparisons

## 2. ACTUATOR DETAILS

Illustrated in Figure 5a, the LaRC-MFC™ actuator consists of three primary components: 1) a sheet of aligned piezoceramic fibers, 2) a pair of thin polymer films etched with a conductive copper electrode pattern on the surface facing the piezoceramic fibers, and 3) an adhesive matrix material, typically structural epoxy. A typical LaRC-MFC™ actuator package, shown in Figure 5b, is 2.25" wide, 3.75" long, and 0.0092" thick, with 0 degree fiber orientation and an average weight of 10.5 grams. The large rectangular pads, located at each end of the electrode bus lines, are tinned with solder prior to final lamination of the package. Nominally, a peak-to-peak actuation strain of approximately 2000 με in the longitudinal direction is possible for a 4 kV peak-to-peak (4000Vpp) voltage cycle, the nominal maximum used with the MFC™.

Illustrated in Figure 6a, active Fiber Composite actuators are comprised of piezoelectric fibers, polymer matrix, and electrodes. PZT fibers are unidirectionally aligned in order to sense and actuate *in-plane* stresses and strains for structural actuation applications. Currently, semi-continuous 250 μm diameter PZT 5A fibers are used. The matrix material is a film adhesive epoxy polymer. A typical AFC actuator package, shown in Figure 6b, is 2" wide, 5.25" long, and 0.013" thick, with a 0 degree fiber orientation and an average weight of 10.8 grams. Electrodes are available on one end. The standard high-field drive level quoted in current and past AFC literature for the 0.045-inch pitch electrodes is a 3000Vpp/600Vdc biased drive signal; occasionally an extended cycle of 4000Vpp/600Vdc (or with higher DC offset) is used. Typical performance at the standard drive level is on the order of 1500 με.

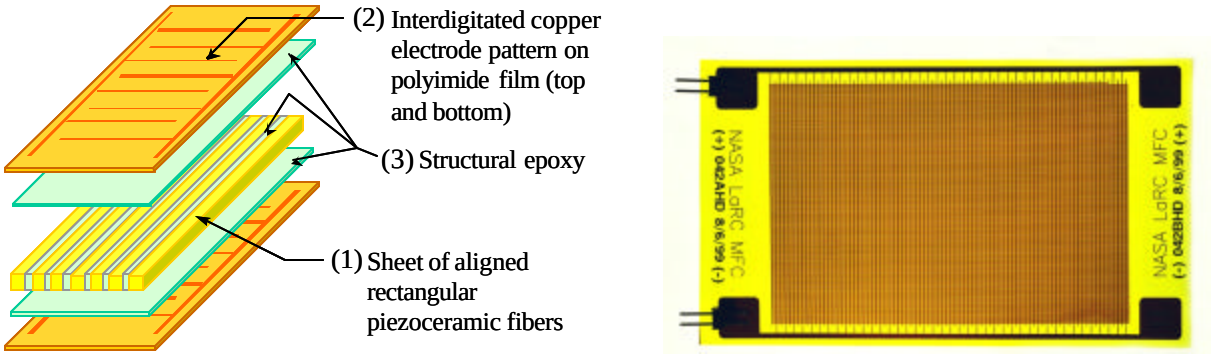


(a) Actuator Components (b) Typical Actuator Package

Figure 5. Langley Macro-Fiber Composite™ Actuator

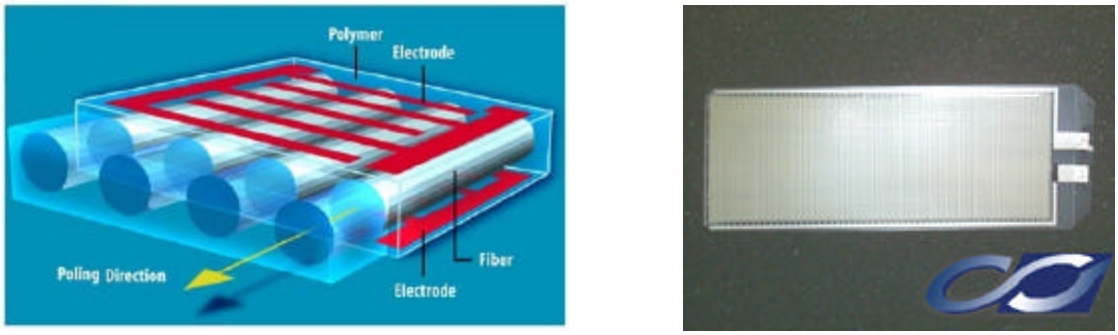


(a) Actuator Components (b) Typical Actuator Package

Figure 6. AFC Actuator (from Reference 18)

## 3. ENABLE TEST ARTICLE

To evaluate these new actuator technologies in a buffet loads environment, an existing F/A-18 model was refurbished for testing in the Transonic Dynamics Tunnel at the NASA Langley Research Center. This 1/6$^{th}$ scale F/A-18 model, shown in Figure 7, was used in previous tests to evaluate the previous generation actuator technologies leading to their full-scale ground test.

Figure 7. 1/6-scale F/A-18 Model Mounted in the Transonic Dynamics Tunnel

Two new fins were manufactured using construction techniques shown in Figure 8. The fin skins consisted of 2 plies of 0.0015-inch thick white fiberglass cloth and an epoxy resin (Figure 8a). The actuators were placed on the inside surface of the inner ply and cured with the skins using molds and in vacuum (Figure 8b). Flexible cables made of copper-clad polyimid

film extended from each actuator to the root of the fin to power the actuators during operation (Figures 8a and 8b). The shape of the fin was maintained by 8-lb foam core (Figure 8c). An aluminum root fitting (Figure 8c) provides attachment to the F/A-18 model following final assembly. Once cured, the skins were bonded to the foam core, yielding the final construction assembly (Figure 8d).

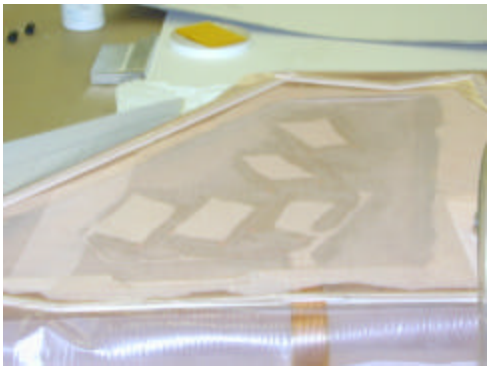

(a) Skins, actuators, and flex cable prior to curing

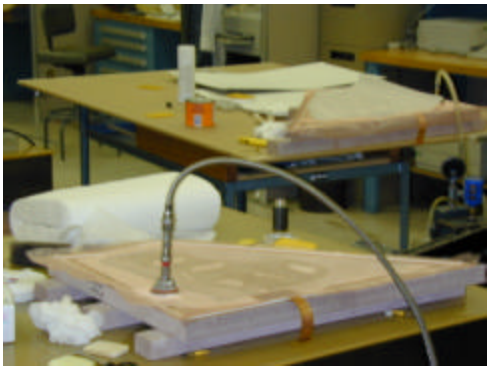

(b) Skin assemblies in molds during curing cycle

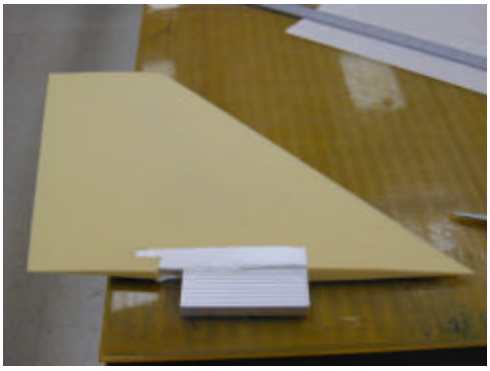

(c) Foam core with root fitting

(d) Final Construction Assembly

Figure 8. Fin Model Construction

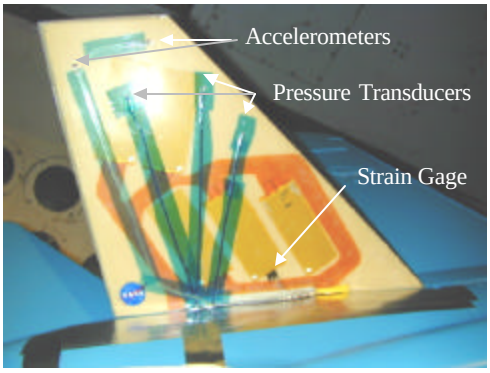


(a) Port-side Fin with AFC Actuators

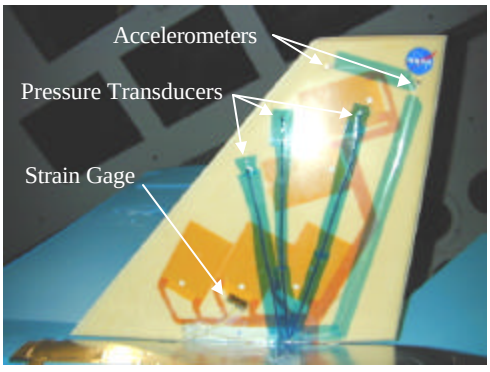


(b) Starboard-side Fin with MFC Actuators

Figure 9. Vertical Fins With Embedded Actuators, Surface Mounted Accelerometers, Pressure Transducers, and Strain Gage, Inboard Surfaces Shown

A total of ten AFC actuators, five per side, are embedded beneath the fiberglass shell of the port fin, shown in Figure 9a. Ten MFC™ actuators, five on each side, are embedded beneath the fiberglass shell of the starboard fin, shown in Figure 9b. Six actuators (3 per side) were placed near the root to alleviate the buffeting in first bending mode. Four actuators (2 per side)

were placed near the tip to alleviate buffeting in the first torsion mode. Accelerometers at the tip and strain gages at the root of the fins measure responses due to commanded inputs to the actuators and the buffet. Pressure gages near the 75% span provide a measure of the buffet. With controllability and observability of the modes in mind, final placement of actuators and instrumentation was based on finite element analysis, planform, actuator and cable dimensions, and knowledge from previous experiments.

## 4. BUFFET LOAD ALLEVIATION SYSTEM DESCRIPTION

Shown in Figure 10, the BLA system used for this test involved a variety of hardware, software, and instrumentation. Starting with the fin, the measured output of each fin was the strain (με) near the root and two accelerations ($g_1$ and $g_2$) at the tip. The strain near the root served as an additional metric for system identification, control law performance, and buffeting alleviation effectiveness of the actuators. After passing through signal conditioners, tip accelerations were fed back through the controller to the control laws ($CLaw_1$ and $CLaw_2$). The control law gains ($K_1$ and $K_2$) could be set separately as shown. When the switches were closed (i.e., feedback is on), the output of the controller ($c_1$ and $c_2$) was sent to the summing junction where it was combined with additional commands ($v_1$ and $v_2$), which were used for system identification, a process described later. As a precaution to prevent damage to the actuators, the input to the voltage amplifiers ($l_1$ and $l_2$) was limited to 1 volt (2 Vpp) using limit switches shown in Figure 10. The voltage amplifiers having fixed internal gains of 1000 were used to drive the piezoelectric actuators. Since the actuators cause motion of the fin through strain actuation, the input to the fin by the actuators is defined by strains $\varepsilon_1$ and $\varepsilon_2$. The other input to the fin is the buffet or unsteady surface pressures described below.

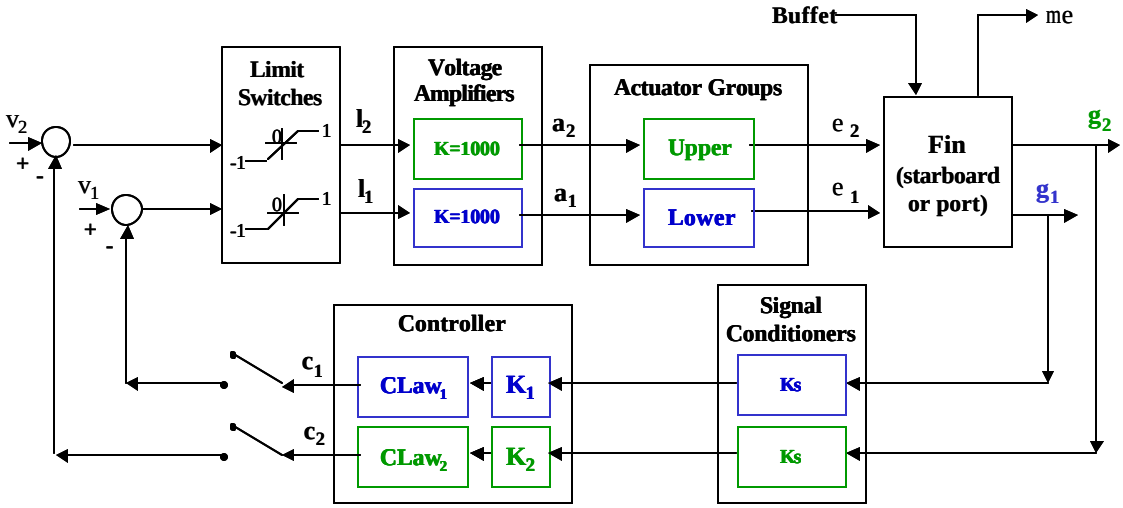


Figure 10. Buffet Load Alleviation System Block Diagram Illustrating Signal Flow During Buffeting Alleviation

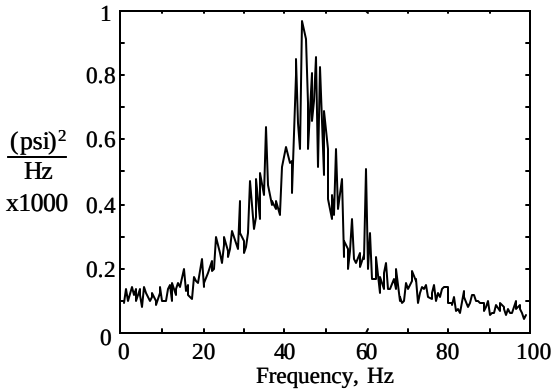


Figure 11. PSD of the Unsteady Pressures on the Inboard/Outboard Surface of the Port/Starboard Fin, Mach 0.11, 25 Degrees Angle of Attack

The unsteady pressures vary with angle of attack and airspeed. Shown in Figure 11 is the power spectral density (PSD) of the unsteady pressures on the surfaces of the fin at Mach 0.11 and 25 degrees angle of attack. For this airspeed and angle of attack, the peak value of the PSD occurs around 45 Hz. With knowledge learned from previous buffet studies, the magnitude and location of the peak value can be changed. From the standpoint of structural dynamics, this understanding is important in that the peak value of the buffet can be placed at a frequency value near a fin's structural mode to maximize response or moved away from the structural frequencies to reduce response.

## 5. SYSTEM IDENTIFICATION

System identification of the fins was conducted for the purpose of control law design. Consistent with previous tests of this F/A-18 model, system identification was performed at high angles of attack between 20 and 38 degrees and Mach numbers between 0 and 0.11. Shown schematically in Figure 10, system identification is performed by calculating frequency responses of output accelerometers ($g_1$ and $g_2$) with respect to excitations ($v_1$ and $v_2$) of the piezoelectric actuator groups. When a loop is open (i.e., feedback is off), then the open-loop dynamics of the fin are identified. When a loop is closed (i.e., feedback is on), then the closed-loop dynamics of the fin are identified. In frequency ranges encompassing each fin's bending and torsion modes, linear sine sweep excitations ($v_1$ and $v_2$) were sent to each actuator group independently while the tip accelerations ($g_1$ and $g_2$) were measured. Frequency response functions were computed from this data.

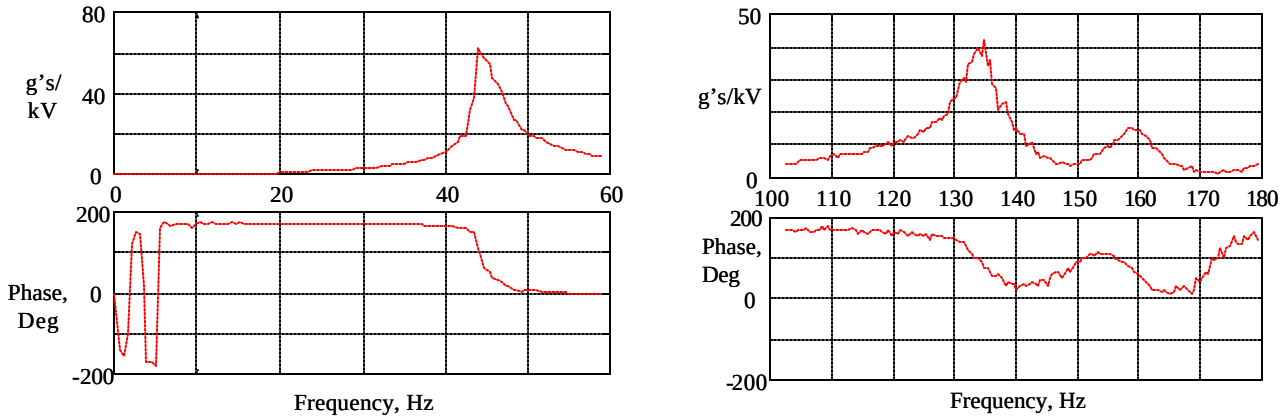


(a) First Bending Mode, Lower MFCs (b) First Torsion Mode, Upper MFCs

Figure 12. Frequency Response Function Indicating First Bending and First Torsion Modes of Starboard-side Fin, Tip Accelerations ($g_1$ and $g_2$) with Respect to Commanded Voltages ($v_1$ and $v_2$) to Lower and Upper MFC Actuators, Respectively, Wind Off, Open Loop

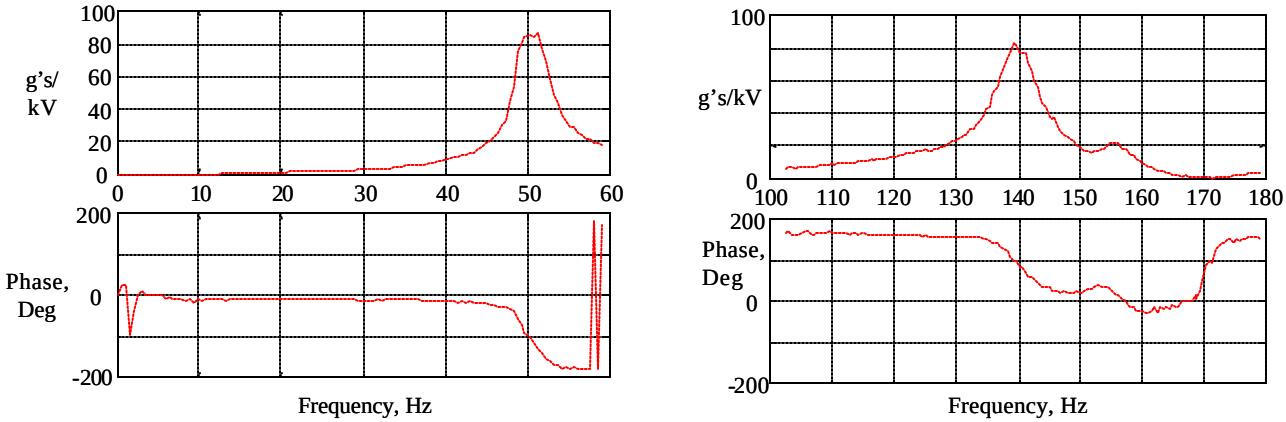


(a) First Bending Mode, Lower AFCs (b) First Torsion Mode, Upper AFCs

Figure 13. Frequency Response Function Indicating First Bending and First Torsion Modes of Port-side Fin, Tip Accelerations ($g_1$ and $g_2$) with Respect to Commanded Voltages ($v_1$ and $v_2$) to Lower and Upper AFC Actuators, Respectively, Wind Off, Open Loop

Shown in Figure 12 for zero airspeed are the frequency response functions of tip accelerations due to command of the MFC actuators on the starboard-side fin. The peak in the magnitude plot of Figure 12a is the first bending mode around 44 Hz. The peak in the magnitude plot of Figure 12b is the first torsion mode around 135 Hz, and the mode around 160 Hz is the fin's second bending mode. The lower MFC actuators when working together are capable of producing about 60 g's of response in the first bending mode per 1000 volts of excitation. The upper MFC actuators when working together are capable of producing about 40 g's of response in the first torsion mode per 1000 volts of excitation.

Similarly, as shown in Figure 13a for the port-side fin, the lower AFC actuators when working together are capable of producing about 85 g's of response in the first bending mode around 50 Hz per 1000 volts of excitation. As shown in Figure 13b, the upper AFC actuators when working together are capable of producing about 80 g's of response in the first torsion mode around 140 Hz per 1000 volts of excitation. The differences in magnitude (force output) shown in Figures 12 and 13 are relative to differences in shape and amount of piezoelectric material in the two types of actuators.

Using these frequency response functions shown in Figures 12 and 13, control laws were designed using frequency domain methods to alleviate buffeting in the first bending and first torsion modes of the fins. Since these modes were well separated, single-input single-output (SISO) controllers could be implemented using some filtering within the control law. Low pass filtering (in $CLaw_1$) and band-pass filtering (in $CLaw_2$) are used so that other modes are not excited when feedback is turned on as well as to concentrate the amplifier energy near the modal frequencies of interest.

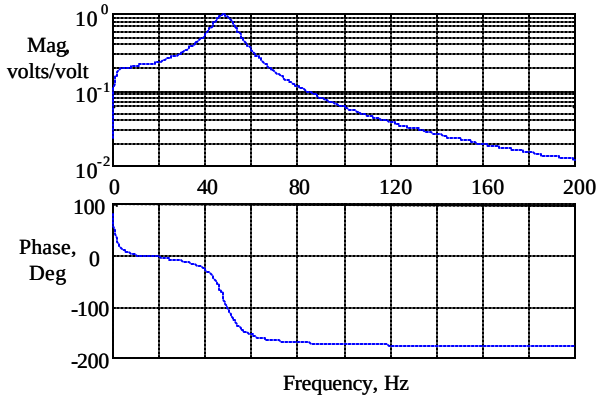


(a) For First Bending Mode Using Lower MFCs, $CLaw_1$

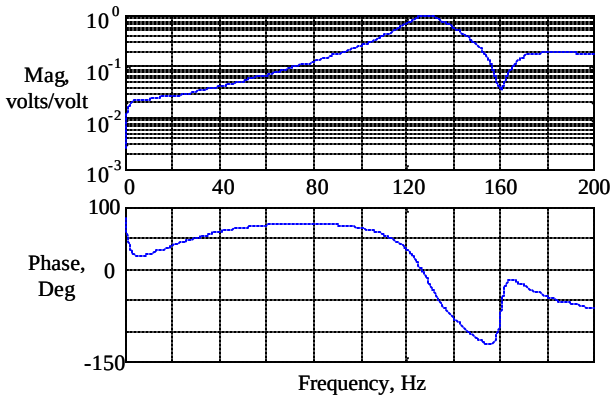


(b) For First Torsion Mode Using Upper MFCs, $CLaw_2$

Figure 14. Frequency Response Functions of Typical Control Laws for Starboard-side Fin, Commanded Voltages ($c_1$ and $c_2$) to Lower and Upper Voltage Amplifiers with Respect to Gained Accelerations ($g_1$ and $g_2$ of Figure 10), Respectively

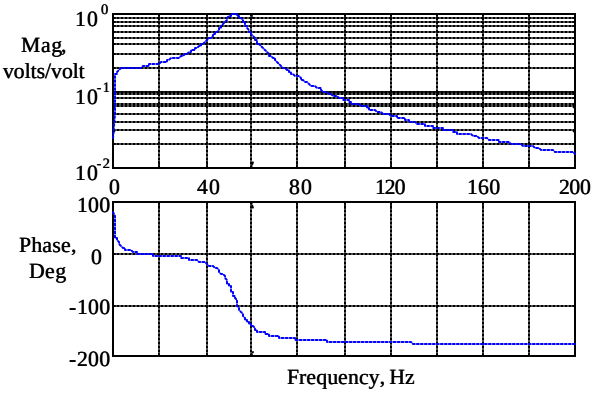


(a) For First Bending Mode Using Lower AFCs, $CLaw_1$

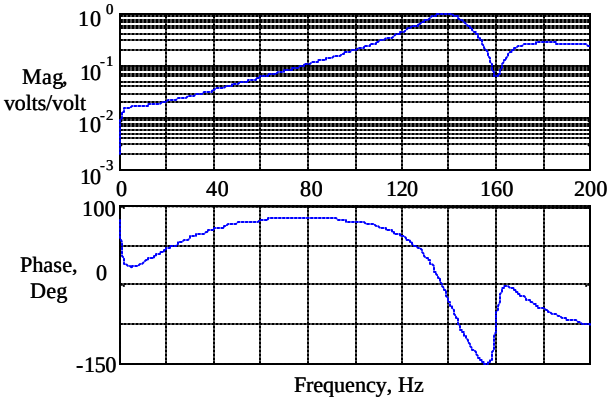


(b) For First Torsion Mode Using Upper AFCs, $CLaw_2$

Figure 15. Frequency Response Functions of Typical Control Laws for Port-side Fin, Commanded Voltages ($c_1$ and $c_2$) to Lower and Upper Voltage Amplifiers with Respect to Gained Accelerations ($g_1$ and $g_2$ of Figure 10), Respectively

Shown in Figures 14a and 14b, in frequency response function form, are the control laws, $CLaw_1$ and $CLaw_2$, used to alleviate buffeting in the first bending and first torsion modes, respectively, of the starboard-side fin. Using a variety of inverse notches and lead-lag compensators, the magnitude and phase could be set at desired values. The peak magnitude of each control law was placed near the frequency of the modal frequency of interest. The peak value was purposely set to unity since adjustments to the magnitude could be made via the gain block ($K_1$ and $K_2$ of Figure 10). The phase of the control law near the modal frequency of interest was set to negative 90 degrees so to augment structural damping.

Similarly, SISO control laws were designed to alleviate buffeting in the first bending and torsion modes of the port-side fin and are provided in frequency response form in Figures 15a and 15b. Prior to sending controller commands to the wind-tunnel model, the control laws were verified and their performance was estimated.

## 6. BUFFETING ALLEVIATION AND ACTUATOR PERFORMANCE RESULTS

After surveying the buffet and buffeting occurring at angles of attack between 20 and 38 degrees and wind-tunnel conditions up to Mach 0.11, the worst case buffeting conditions were found to occur around 25 degrees angle of attack for the higher Mach numbers. Testing was concentrated near these wind-tunnel and model conditions. Thirty variations of the control laws were tested. The power spectral density (PSD) functions of tip accelerations were used to compare open-loop (feedback off) and closed-loop (feedback on) buffeting for evaluating the performance of each control law, which, in turn, provided an evaluation of the new actuators.

Shown in Figures 16a and 16b for the starboard-side fin at Mach 0.105 and 25 degrees angle of attack, the peak magnitude of the closed-loop (feedback on) buffeting is considerably and desirably lower than the peak open-loop (feedback off) buffeting for frequencies near the first bending and torsion modes, respectively. Using a maximum input command of 1000 volts to the lower MFC actuators, peak acceleration in the first bending mode was reduced about 70% (Figure 16a). The root mean square (RMS) values of tip acceleration were reduced about 30%. Shown in Figure 16b, peak acceleration in the first torsion mode was reduced about 40% when using about 111 volts (RMS). The increase in magnitude around 125 Hz is caused by the control law and could have been prevented through proper adjustment of the phase in that region of the spectra.

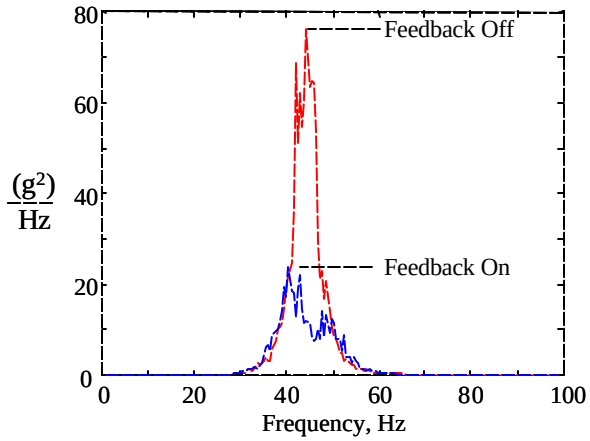


(a) Using Feedback Control to Lower MFC Actuators

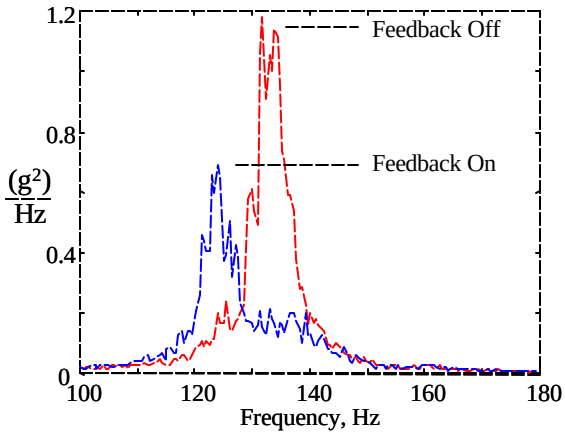


(b) Using Feedback Control to Upper MFC Actuators

Figure 16. PSDs of Tip Acceleration for Feedback Off and On Cases, Starboard-side Fin, Mach 0.105, 25 Degrees Angle of Attack

Similar buffeting alleviation results were observed during BLA operation of the AFC actuator groups on the port-side fin. Shown in Figures 17a and 17b for the port-side fin at Mach 0.105 and 25 degrees angle of attack, the peak magnitude of the closed-loop (feedback on) response is considerably and desirably lower than the peak open-loop (feedback off) response for frequencies near the first bending and torsion modes, respectively. Using a maximum input command of 1000 volts to the lower AFC actuators, peak acceleration in the first bending mode was reduced about 85% (Figure 17a). RMS values of tip acceleration were reduced about 40%. Shown in Figure 17b, peak acceleration in the first torsion mode was reduced about 30% when using about 32 volts (RMS). As was the case for the upper MFC actuator group, the increase in magnitude around 135 Hz (Figure 17b) is caused by the control law and could have been prevented through proper adjustment of the phase in

that region of the spectra. However, because buffeting in the first torsion mode is substantially less than the buffeting in the first bending mode, no additional effort was spent on adjusting those control laws ($CLaw_2$).

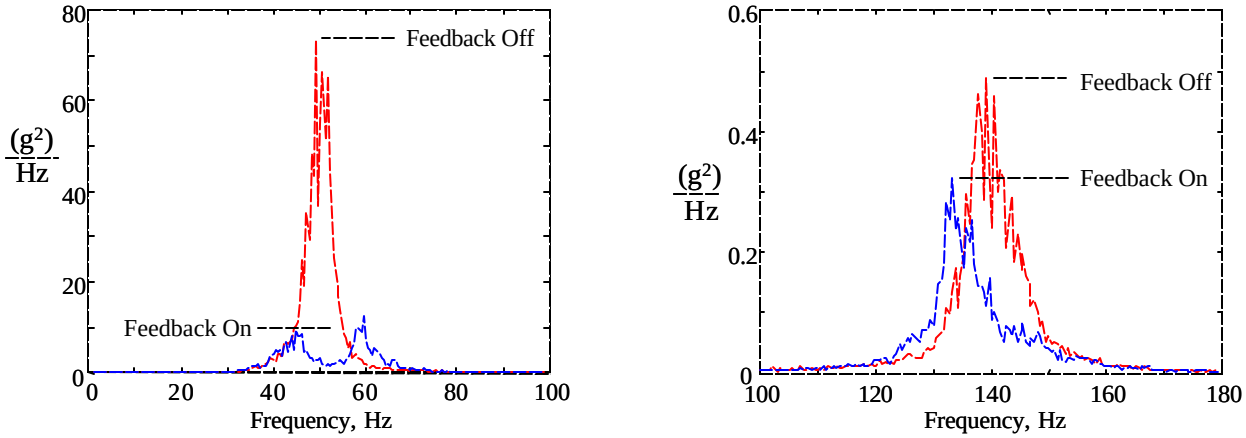


(a) Using Feedback Control to Lower AFC Actuators (b) Using Feedback Control to Upper AFC Actuators

Figure 17. PSDs of Tip Acceleration for Feedback Off and On Cases, Port-side Fin, Mach 0.105, 25 Degrees Angle of Attack

BLA performance was measured at other Mach numbers while the model was set at 25 degrees angle of attack. At Mach numbers lower than 0.105, the buffeting in the first bending mode was lower, as illustrated by the columns designated "OL" in Figures 18 and 19. The reason that the buffeting is less for the lower Mach numbers can be explained by further consideration of the buffet spectra identified in Figure 11. As Mach number is reduced from the value of 0.105, the peak magnitude shown around 45 Hz will move to a lower frequency as well as a lower value. From a structural dynamics point of view, when the Mach number is reduced, the frequency of the peak value moves away from the frequency of the structural modes, thus reducing modal response. This effect not only explains why the buffeting in the first torsion mode is much lower than the buffeting in the first bending mode, but also suggested a parametric study of buffeting alleviation in the first bending mode. Thus, a parametric study of BLA performance was conducted for the lower actuator group of each fin. Using several values of feedback gain ($K_1$ of Figure 10), the tip accelerations in the first bending modes of each fin were reduced and their respective amplifier drive voltages (RMS) noted beneath each "CL" column in Figures 18 and 19. Consistent with previous tests, the PSD value of the buffeting in a structural mode is used. For voltage amplifiers, the RMS value is used since it implies an output voltage requirement to drive these actuators. To achieve the alleviation results at Mach 0.105 (PSDs shown in Figures 16a and 17a), the amplifier drive voltages to the lower MFC and lower AFC actuator groups were 544 volts (RMS) and 530 volts (RMS), respectively. Higher feedback gains could have been used; however, with the input voltage to the actuators limited to +/-1000 volts, significant signal clipping would have hindered an accurate measure of performance. Using this limited input, less than 50% of the actuators' capacity was used in providing the reductions shown in Figures 18 and 19.

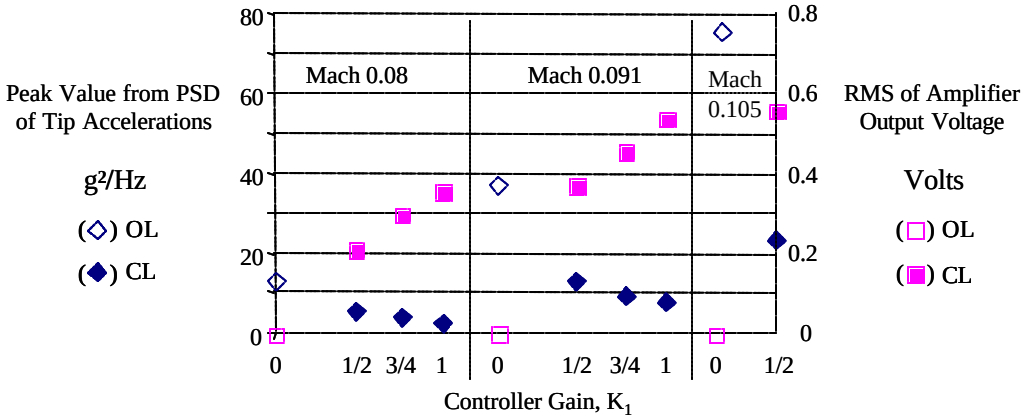


Figure 18. Peak Values from PSD of Tip Acceleration, Near Frequency of First Bending Mode, Starboard-side Fin, Lower MFC Actuator Group, For Three Mach Numbers, 25 Degrees Angle of Attack

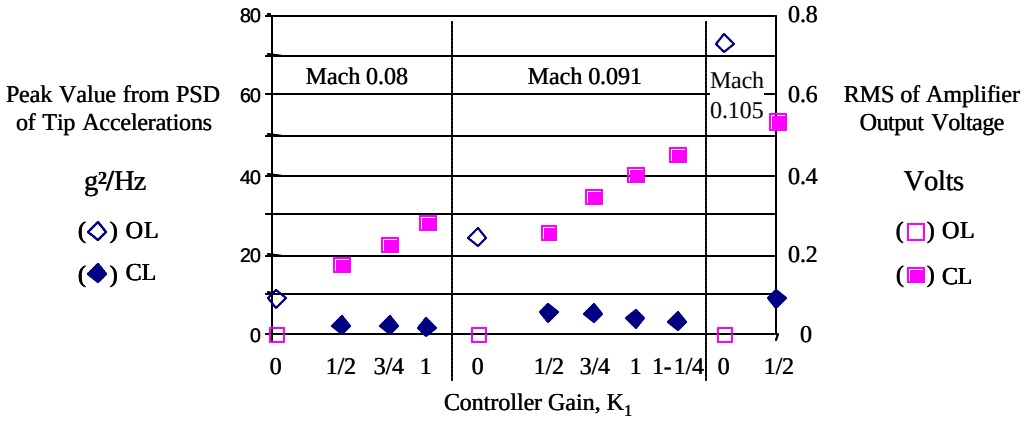


Figure 19. Peak Values from PSD of Tip Acceleration, Near Frequency of First Bending Mode, Port-side Fin, Lower AFC Actuator Group, For Three Mach Numbers, 25 Degrees Angle of Attack

Prior to completion of the test, several failure modes of the actuators were observed during this test when the voltage limits to the actuators were accidentally exceeded in the form of a voltage spike well above standard operational levels. The MFC actuators showed no visible signs of damage but were unpoled by the negative high voltage. Repoling was performed in situ to restore performance. The AFC actuators suffered more damage, as shown in Figure 20, since they experienced a larger voltage spike. However, repair to the AFC actuator was possible by isolating the damaged region from the electrical bus. To isolate the damaged region, the regions of IDEs, circled in Figure 20b, were severed intentionally, and the resulting gaps were filled with a non-conductive material to prevent electrical arching. This repair was possible because the damaged region was visible and accessible. Following the poling of the MFC actuators and the repair of the AFC actuator, testing resumed using all MFC and AFC actuators.

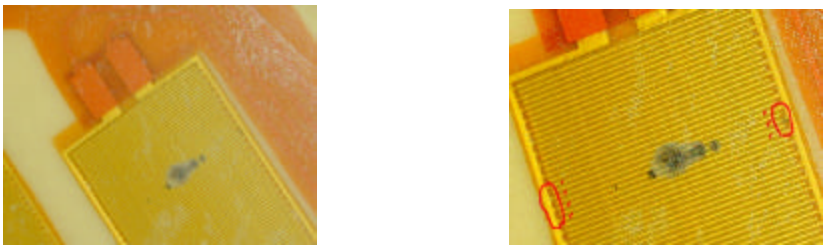

(a) Damaged Region of an AFC Actuator (b) Regions of IDEs Identified for Repair

Figure 20. Damaged Region and Repair of Damaged AFC Actuator

## 7. CONCLUSIONS

As demonstrated herein, the AFC actuator developed by Continuum Control Corporation and the MFC actuator developed by the NASA Langley Research Center performed similarly and superbly in reducing structural responses caused by buffet. Based on the test results presented herein, both actuators look promising for use during full-scale ground and flight tests being planned by the USAF, Boeing, and NASA. Based on observations, one noticeable deterrent to using these IDE devices if embedded in operational aerospace vehicles is the limited accessibility in case of repair. For this test, repair was possible because the actuator was accessible through the transparent skin of the fin. Also noteworthy are the high (KV range) voltages required to drive these actuators. As in the past, full-scale investigations could lead to additional trade studies for finding a workable compromise in terms of fatigue life enhancement versus demands on vehicle subsystems. The experimental data and results of this test provide a valuable baseline for understanding the system-level architecture required to integrate a buffeting alleviation system into future operational aerospace vehicles.

## 8. ACKNOWLEDGMENTS

The authors would like to extend their deepest gratitude to the following personnel at the NASA Langley Research Center: Richard Chattin and James Linker of the Materials Resources and Instrumentation Section for fabricating the two fins, to

Tom Vranas of the Computer Aided Technologies Section for designing and fabricating the molds, to Johnny Mau of the Microelectronics & Technology Support Section for designing and procuring the flexible cables, to James High of the Microelectronics & Technology Support Section for manufacturing the MFC actuators, to David Coulson of Wyle for programming the digital controller, to the staff at the Transonic Dynamics Tunnel who assisted with model preparations, testing, BLA system repair, and data processing, and to Keats Wilkie for the MFC actuator characteristics stated herein.

## 9. REFERENCES

1 Triplett, W. E., "Pressure Measurements on Twin Vertical Tails in Buffeting Flow," AFWAL-TR-82-3015, Vols I & II, prepared for USAF Flight Dynamics Laboratory, April 1982.

2 Triplett, W. E., "Pressure Measurements on Twin Vertical Tails in Buffeting Flow," J. Aircraft, Vol. 20, No. 11, November 1983, pp. 920-925.

3 Zimmerman, N. H., and Ferman, M. A., "Prediction of Tail Buffet Loads for Design Application," Vols. I and II, Rept. No. NADC-88043-60, July 1987.

4 Lee, B. H. K., Brown, D., Zgela, M., and Poirel, D., "Wind Tunnel Investigation and Flight Tests of Tail Buffet on the CF-18 Aircraft", AGARD-CP-483, Advisory Group for Aerospace Research and Development Specialist's Meeting, Sorrento, Italy, April 1990.

5 Shah, G. H., "Wind-Tunnel Investigation of Aerodynamic and Tail Buffet Characteristics of Leading-Edge Extension Modifications to the F/A-18," AIAA Atmospheric Flight Mechanics Conference, AIAA 91-2889, New Orleans, LA, August 12-14, 1991.

6 Pettit, C. L., Banford, M., Brown, D., and Pendleton, E., "Full-Scale Wind-Tunnel Pressure Measurements on an F/A-18 Tail During Buffet," Journal of Aircraft, Vol. 33, No. 6, November-December 1996, pp. 1148-1156.

7 Meyn, L. A. and James, K. D., "Full-Scale Wind-Tunnel Studies of F/A-18 Tail Buffet," Journal of Aircraft, Vol. 33, No. 3, May-June 1996, pp. 589-595.

8 Moses, R. W. and Pendleton, E., "A Comparison of Pressure Measurements Between a Full-Scale and a 1/6-Scale F/A-18 Twin Tail During Buffet," 83rd Structures and Materials Panel Meeting, AGARD-R-815, Loads and Requirements for Military Aircraft, 2-6 September 1996, Florence, Italy.

9 Moses, R.W. and Ashley, H., "Spatial Characteristics of the Unsteady Differential Pressures on 16% F/A-18 Vertical Tails," AIAA-98-0519, 36th AIAA Aerospace Sciences Meeting and Exhibit, Reno, Nevada, January 12-15, 1998.

10 Moses, R. W. and Shah, G. H., "Spatial Characteristics of F/A-18 Vertical Tail Buffet Pressures Measured in Flight," AIAA-98-1956, 39th AIAA/ASME/ASCE/AHS/ASC Structures, Structural Dynamics, and Materials Conference and Exhibit, Long Beach, CA, April 20-23, 1998.

11 Moses, R. W., Huttsell, L., FIN BUFFETING FEATURES OF AN EARLY F-22 MODEL, AIAA 2000-1695, 41st AIAA/ASME/ASCE/ASC Structures, Structural Dynamics, and Materials Conference and Exhibit, Atlanta, GA, April 2000.

12 Ashley, H., Rock, S. M., Digumarthi, R., and Chaney, K., "Further Study of Active Control for Fin Buffet Alleviation, With Application to F-22," WL-TR-97-3073, July 1997.

13 Moses, Robert W., Active Vertical Tail Buffeting Alleviation on a Twin-Tail Fighter Configuration in a Wind Tunnel, CEAS International Forum on Aeroelasticity and Structural Dynamics 1997, Rome, Italy, June 17-20, 1997, pp. 8.

14 Moses, Robert W., NASA Langley Research Center's Contributions to International Active Buffeting Alleviation Programs, NATO-RTO Workshop on Structural Aspects of Flexible Aircraft Control, Ottawa, Canada, October 18-21, 1999.

15 Ryall, T., Moses, R., Hopkins, M., Henderson, D., Zimcik D., Nitzsche, F., Buffet Load Alleviation, Second Australasian Congress on Applied Mechanics, Canberra, Australia, February 10-12, 1999.

16 Nitzsche, F., Zimcik, D., Ryall, T., Moses, R., Henderson, D., Control Law Synthesis for Vertical Fin Buffeting Alleviation Using Strain Actuation, 40th AIAA/ASME/ASCE/AHS/ASC Structures, Structural Dynamics, and Materials Conference, St. Louis, Missouri, AIAA 99-1317, April 12-15, 1999.

17 Wilkie, W. K., Bryant, R. G., High, J. W., Fox, R. L., Hellbaum, R. F., Jalink, A., Jr., Little, B. D., and Mirick, P. H., Low-Cost Piezocomposite Actuator for Structural Control Applications, SPIE's 7th Annual International Symposium on Smart Structures and Materials, Newport Beach, CA, March 5-9, 2000.

18 Bent, A. A, Pizzochero, A. E., Recent Advances in Active Fiber Composites for Structural Control, SPIE's 7th Annual International Symposium on Smart Structures and Materials, Newport Beach, CA, March 5-9, 2000.

19 Bent, A. A., "Active Fiber Composite Material Systems for Structural Control Applications," *Proceedings, SPIE's 6th International Symposium on Smart Structures and Materials*, Newport Beach, CA, March 1-5, 1999.